Available online at www.sciencedirect.com

ScienceDirect

Ceramics International 42 (2016) 2750–2760

CERAMICS INTERNATIONAL

www.elsevier.com/locate/ceramint

Producing dense zirconium diboride components by room-temperature injection molding of aqueous ceramic suspensions

Valerie L. Wiesner[a,*,1], Lisa M. Rueschhoff[b], Andres I. Diaz-Cano[b], Rodney W. Trice[b], Jeffrey P. Youngblood[b]

[a]NASA Glenn Research Center, Cleveland, OH 44135, USA
[b]School of Materials Engineering, Purdue University, West Lafayette, IN 47907, USA

Received 3 September 2015; received in revised form 19 October 2015; accepted 2 November 2015
Available online 14 November 2015

Abstract

Aqueous suspensions of zirconium diboride (ZrB_2), boron carbide (B_4C) and tungsten carbide (WC) with dispersant and water-soluble polyvinylpyrrolidone (PVP) were investigated for processing by room-temperature injection molding, a novel, environmentally benign ceramic processing method. B_4C and WC were used as sintering aids, and the as-received powders were attrition milled to reduce particle size to promote full densification of ZrB_2 specimens by pressureless sintering. Zeta potential measurements of individual ZrB_2, B_4C and WC powders and of powder mixtures revealed that maximum stability was achieved in aqueous solutions of attrition milled powder mixtures dispersed using an ammonium polyacrylate dispersant. A maximum powder loading of 49 vol% with ≤ 5 vol% PVP was attained for $ZrB_2/B_4C/WC$ suspensions with dispersant. Although exhibiting a time-dependent rheological response determined by parallel-plate rheometry, suspensions containing 49 vol% powders and ≤ 3 vol% PVP, as well as suspensions of 46 vol% powders and ≤ 4 vol% PVP, were flowable under the conditions of the process. ZrB_2 rings prepared by room-temperature injection molding were machinable prior to binder removal and exhibited maximum brown densities of 56% true density (TD). Sintered densities were >98%TD with ~ 20% linear shrinkage. Scanning electron microscopy revealed an average grain size of 7.3 ± 2.8 μm, and chemical analysis confirmed that no undesirable oxide phases remained in the sintered ZrB_2 specimens. Aqueous ZrB_2-based suspensions containing B_4C and WC sintering aids and PVP were effectively processed via room-temperature injection molding to yield dense ZrB_2 rings after binder burnout and pressureless sintering.
Published by Elsevier Ltd and Techna Group S.r.l.

Keywords: Injection molding; Borides; Suspensions

1. Introduction

New technologies, particularly in aerospace, that involve design and manufacture of complex-shaped ceramic components have burgeoned in recent decades [1,2]. The development of advanced hypersonic and re-entry vehicles requires materials resistant to erosion and oxidation along with the ability to withstand operating temperatures well above 2000 °C that are routinely encountered in the severe re-entry environment [3]. Zirconium diboride (ZrB_2), an ultra-high temperature ceramic (UHTC), is an ideal candidate for these particular applications, due to its combination of high melting temperature (>3000 °C), high thermal conductivity, low density and exceptional strength [4,5]. The capability to form components with complex geometries is the next step in development of UHTCs for employment in aerospace and beyond.

Because ZrB_2 typically exhibits low volume and grain boundary diffusion rates, high temperatures are required to

*Corresponding author. Tel.: +1 216 433 5427; fax: +1 216 433 5544.
E-mail address: valerie.l.wiesner@nasa.gov (V.L. Wiesner).

[1]Presented in part at the 36th International Conference on Advanced Ceramics and Composites, Daytona Beach, FL, January 2014. Based in part on the dissertation submitted by V.L. Wiesner for the Ph.D. degree in Materials Engineering, Purdue University, West Lafayette, Indiana (2013).

http://dx.doi.org/10.1016/j.ceramint.2015.11.005
0272-8842/Published by Elsevier Ltd and Techna Group S.r.l.

sinter parts to full density without sintering aids [6]. Dense ZrB_2 components have been traditionally prepared by hot-pressing at high temperatures ($>2000\ ^{\circ}C$) with moderate pressures (~ 30 MPa) or at lower temperatures (1800 °C) with very high pressures (>800 MPa) [7]. Although an effective and repeatable densification method, hot-pressing cannot effectively sinter ceramic components with complex geometries in a high-throughput manner suitable for widespread application [8]. Conventional densification methods for UHTCs, like hot pressing [9] or spark plasma sintering [10], cannot economically produce the complex-shaped components (i.e. highly curved leading wing-edges for hypersonic vehicles, rocket nozzle-inserts and re-entry vehicle nose cones) needed for aerospace applications without extensive machining [4].

With pressureless sintering, near-net shape production of complex-shaped parts and a reduction in post-processing costs are possible, making it a more appealing densification method for UHTCs. Pressureless sintering of UHTCs, including ZrB_2, has proven to be a challenge in the development and application of these advanced materials mainly due to unavoidable oxygen impurities that exist on the surface of starting powders [7]. These oxygen impurities manifest themselves in the form of boria (B_2O_3) and zirconia (ZrO_2) in the case of ZrB_2, and in their liquid and vapor form at relatively low temperatures ($\sim 1750\ ^{\circ}C$). Their presence enhances grain coarsening by increasing surface diffusion paths. As a result, these surface oxides further reduce the driving force to sinter in ZrB_2 samples, impeding full densification [11].

The effects of these surface impurities have been somewhat mitigated by incorporating a low-temperature heat treatment ($\sim 1340\ ^{\circ}C$) during the pressureless sintering procedure to remove by evaporation the boria phase, which limits grain growth. In order to remove the more complicated metal oxide, a successful approach to pressureless sinter ZrB_2 has involved adding a secondary phase to preferentially react with ZrO_2. Zhang et al. [12] and Fahrenholtz et al. [13] used attrition milling with tungsten carbide (WC) milling media to reduce ZrB_2 powder size to promote densification, as well as to introduce ~ 8 wt% WC into the system. 4 wt% boron carbide (B_4C) was also added to favorably react with ZrO_2 on the surface of ZrB_2 [12,13]. Consequently, these studies were able to achieve $>98\%$ dense ZrB_2 billets after pressureless sintering for only 1 h at 1850 °C [12] and $\sim 100\%$ relative density in ZrB_2 pellets after 2 h at 1850 °C [13], both in an argon atmosphere. Processing methods that employ sintering aids, namely tungsten carbide (WC) and boron carbide (B_4C) [12,13], have effectively reduced the pressureless sintering temperatures ($<2000\ ^{\circ}C$) required to densify ZrB_2 ceramics and composites without significant mechanical property losses [13].

These advances in pressureless sintering have paved the way for ZrB_2 production via colloidal near-net shaping methods, including extrusion, tape casting and gelcasting. Extrusion and tape casting by aqueous and non-aqueous routes have found relative success in producing dense ZrB_2 components; however, the geometries have been restricted by use of hot pressing or sintering at temperatures $>2000\ ^{\circ}C$ to achieve full densification [14,15]. These methods traditionally employ complex binders based on harsh chemical solvents, like toluene and methyl ethyl ketone, in combination with multiple plasticizers [15–17]. Although aqueous-based systems for tape casting and gelcasting of ZrB_2 have been studied recently, these processes require multicomponent binders and/or have not produced dense components without hot pressing or pressureless sintering at temperatures above 2000 °C [18–22].

An aqueous solution of 40% ammonium polyacrylate (PAA-NH_4) with low toxicity [23] has been observed to effectively disperse aqueous, highly loaded (≥ 45 vol%) ZrB_2-based suspensions [18,24]. Ammonium polyacrylate typically promotes stability of aqueous ceramic systems by PAA adsorbing to the surface of ceramic particles to enhance electrosteric stabilization [25]. The ionic dispersant has a molecular weight of 3500 g/mol and is highly soluble in water-based systems [26]. Polyvinylpyrrolidone (PVP) with varying average molecular weights, in combination with a dispersant of either ammonium polyacrylate [27] or of poly(methacrylic acid) ammonium salt (PMAA-NH_4) [28], has been observed to be an effective rheological modifier in aqueous alumina suspensions. Aqueous, PVP-based alumina suspensions dispersed with ammonium polyacrylate have been shown to enable room-temperature injection molding, which is a novel low-cost and low-toxicity ceramic process. This alternate processing method utilizes the flow properties of highly loaded ceramic suspensions to fabricate near-net shape ceramic components without the use of multicomponent binders, harsh crosslinking or curing agents or further chemical processes [27], as well as additive manufacturing [29]. In the current study, room-temperature injection molding was investigated as a water-based, alternative process to effectively produce dense near-net shape zirconium diboride parts.

2. Experimental approach

2.1. Materials

The ceramic powders used to prepare ZrB_2-based suspensions were ZrB_2 powder (Grade B, H.C. Starck, Newton, MA) and B_4C powders (Grade HS, H.C. Starck, Newton, MA) with an average particle size of 2–4 μm and 0.8 μm, respectively. Tungsten carbide powders (product no. 12482, Alfa Aesar, Ward Hill, MA) with as-received particle size <1 μm were used for zeta potential analysis. 4 wt% B_4C powder was combined with the as-received ZrB_2 powders, and the powder mixture was then attrition milled at 600 RPM in 200-proof ethanol using 1/8″-diameter Co-bonded WC media satellites (Union Process, Akron, OH) for 2 h. The mass of the milling media was weighed before and after attrition milling to estimate the amount of WC introduced into the system. The powders were then dried at 70 °C on a hot stir plate. To break up any agglomerates formed during the drying process, the dried powders were dry ball milled for 24 h using 1/2″-diameter WC satellite media. A final drying step in a box furnace for 12 h at 100 °C in air was performed to remove any moisture from the powders. The average particle size was estimated by measuring 100 random particles in five different

scanning electron microscopy (SEM) micrographs of the powders before and after attrition milling. Powder X-ray diffraction (XRD) analysis (0.02° step, 2.5 s/step) using a Bruker D8 Advance diffractometer with Cu Kα radiation was employed to evaluate the phase composition of the attrition milled powders. Chemical composition of the attrition milled powders was performed by NSL Analytical Services, Inc. (Cleveland, OH) to quantitatively ascertain boron and tungsten contents using inductively coupled plasma optical emission spectrometry (ICP-OES), carbon and oxygen contents by a Leco Furnace method and zirconium content by difference after the impurities scan.

Darvan 821A (aqueous solution of 40% ammonium polyacrylate (PAA-NH_4), R.T. Vanderbilt Company, Inc., Norwalk, CT) was used as a dispersant. Polyvinylpyrrolidone (PVP, 1-ethenyl-2pyrrolidinone homopolymer, Sigma-Aldrich, St. Louis, MO) with average molecular weight of 10,000 g/mol was used as a binder to tailor the rheological properties of the aqueous ZrB_2-based suspensions.

2.2. Suspension preparation

Suspensions were prepared by combining a slurry of deionized (DI) water, dispersant and attrition milled ZrB_2, B_4C and WC powders and ball milling in 8 oz. Nalgene bottles with 1/4″-diameter WC satellite milling media. The attrition milled ZrB_2, B_4C and WC powders were incrementally added to the dispersant and DI water solution to obtain dispersed slurries. A typical slurry contained 330 g of powder in ~40 to 50 mL of DI water and ~9 mL dispersant. A polymer solution of PVP with average molecular weight of 10,000 g/mol and DI water was mixed separately by magnetic stirring for 4–8 h. After both the slurry and polymer solution were dispersed, the PVP-water mixture was added to the ZrB_2-based slurry and ball milled at ~55 rotations per minute over a 12-hour period.

The compositions of ZrB_2-based suspensions studied with related nomenclature are highlighted in Table 1. The concentrations of PVP in suspensions with 46 and 49 vol% attrition milled powders and ~7 vol% dispersant, which corresponded to an ammonium polyacrylate concentration of approximately 2 mg/m^2, were varied from 0 to 5 vol% in order to determine the optimal content that resulted in favorable forming and specimen properties, including density and chemical composition, after binder burnout and pressureless sintering.

2.3. Room-temperature injection molding process

A schematic of the room-temperature injection mold device is shown in Fig. 1. The mold cavity was devised to yield a ring-shaped part. Producing a ceramic specimen in the shape of a ring was desired over preparing a sample with a more common and basic geometry, such as a bar or disc, in order to investigate and resolve processing obstacles, which included convergent flow effects encountered during filling of the mold that could cause pore or defect development and the formation

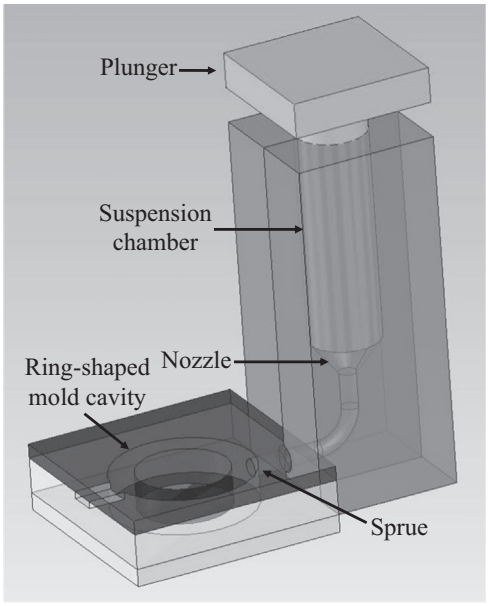

Fig. 1. Graphic representation of room-temperature injection mold apparatus.

Table 1
Suspension compositions with stresses required to initiate flow and average densities and grain sizes of resulting ZrB_2 specimens.

Suspension name	Amount of ZrB_2/B_4C/WC powder content in vol% (wt%)	PVP content in vol% (wt%)	Dispersant content in vol% (wt%)	Stress initiating flow (Pa)	Average green bulk density in g/cm^3 (% TD)	Average sintered bulk density in g/cm^3 (% TD)	Average grain size (μm)
46Z-0P	46(84)	0(0)	6.6(2.3)	187	–	–	–
46Z-1P	46(84)	1(0.4)	6.6(2.3)	52	3.28 ± 0.05(53)	6.11 ± 0.05(99)	7.3 ± 2.3
46Z-2P	46(84)	2(0.7)	6.6(2.3)	160	3.30 ± 0.04(53)	5.97 ± 0.11(97)	7.0 ± 2.2
46Z-3P	46(84)	3(1.1)	6.6(2.3)	199	3.28 ± 0.01(53)	6.08 ± 0.05(98)	7.2 ± 1.8
46Z-4P	46(84)	4(1.4)	6.6(2.3)	251	3.31 ± 0.01(54)	6.07 ± 0.01(98)	7.1 ± 2.0
46Z-5P	46(84)	5(1.8)	6.6(2.3)	1000	–	–	–
49Z-0P	49(85)	0(0)	7.0(2.3)	389	–	–	–
49Z-1P	49(85)	1(0.5)	7.0(2.3)	567	3.43 ± 0.03(56)	6.13 ± 0.02(99)	7.4 ± 3.6
49Z-2P	49(85)	2(0.7)	7.0(2.3)	405	3.40 ± 0.03(55)	6.20 ± 0.02(100)	7.4 ± 3.5
49Z-3P	49(85)	3(1.0)	7.0(2.3)	235	3.41 ± 0.06(55)	6.06 ± 0.05(98)	7.7 ± 3.7
49Z-4P	49(85)	4(1.4)	7.0(2.3)	637	–	–	–
49Z-5P	49(85)	5(1.7)	7.0(2.3)	1100	–	–	–

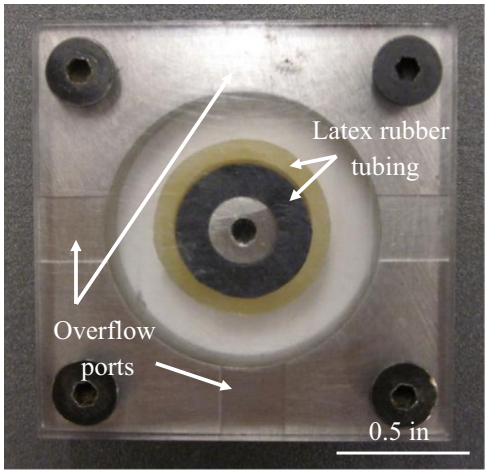

Fig. 2. Ring-shaped mold with centerpiece of super soft black and yellow latex rubber tubing supported by steel post on bottom plate and three overflow ports machined into the steel outer ring support. Plexiglas top plate was secured to the mold with four screws. (For interpretation of the references to color in this figure legend, the reader is referred to the web version of this article.)

of hoop stresses that arose during solidification and drying that could result in cracking of a ceramic ring after injection molding [30].

The dimensions of the mold, shown in Fig. 2, were designed to produce a ring that, prior to binder burnout and sintering, had 2.54-cm outer diameter (OD), 1.59-cm inner diameter (ID) and width of 6.35 mm. Three overflow ports were incorporated into the mold design to allow excess material to flow out of the mold during processing. Both the bottom plate and the outer ring support with injection port were machined from steel. A cylindrical post with a diameter and height of 6.35 mm was inserted through the center of the bottom plate to support an inner ring of super soft black latex rubber tubing (6.35 mm ID, 1.27-cm OD) and an outer ring of soft yellow latex rubber tubing (1.27-cm ID and 1.59-cm OD) from McMaster-Carr (Elmhurst, IL). The yellow outer latex and inner black latex tubes had a firmness of 10 psi and 30 psi at 25% deflection (shore A35), respectively. A transparent Plexiglas material was used for the top plate. The Plexiglas top plate and steel bottom plate of the mold that came in contact with the suspensions during filling were covered with low-friction Teflon tape (McMaster-Carr, Elmhurst, IL) and Grade 40 ashless filter paper (Whatman, UK) to expedite demolding and cleaning of molds. Four screws were used to fasten the top and bottom plates above and below the outer ring support to create the mold cavity. The mold cavity was then secured to the suspension chamber using two screws fitted through the chamber into the steel outer ring support. A 3.175-mm-diameter rubber O-ring was positioned between the mold and chamber to ensure a tight connection. The resulting sprue through which the suspension flowed into the mold cavity from the suspension chamber had a diameter of 3.175 mm.

The inner surfaces of the mold cavity and chamber were lubricated with Liquid Wrench L312 Teflon spray (Indian Trail, NC) to assist in demolding of the ceramic part after forming. The chamber was filled with approximately 5 mL of the ZrB_2-based suspension. After a cylindrical steel pushrod with a diameter of 1.27 cm was inserted into the cylindrical chamber with the same diameter, the injection molding apparatus was placed between compression platens in an electromechanical test frame (MTS Insight 100 load frame, MTS Systems Corporation, Eden Prairie, MN). A compression force at a 75 mm/min crosshead speed was applied to a 1.27-cm diameter ball bearing on top of the pushrod to ensure that the load was uniformly transferred to the pushrod. The force that was consequently exerted onto the suspension at a constant rate was sufficient to initiate flow of the suspension, causing the suspension to fill the mold cavity yielding a ZrB_2 ring. In order to prevent closed pore formation due to air bubbles developing within the suspension during filling, a VM-25 miniature air piston vibrator (Cleveland Vibrator Co., Cleveland, OH) that had a frequency of 16,000 vibrations per minute at 80 psi was secured to the top of the mold cavity using cable ties and activated for the duration of the injection molding operation. Immediately after forming, the Plexiglas plate was removed to allow the resulting ceramic part to dry at ambient conditions for 1 h before removing it from the mold.

2.4. Binder burnout and pressureless sintering

Binder burnout and pressureless sintering were combined into one heat treatment, which was accomplished in a Centorr Vacuum Industries high-temperature controlled environment furnace (Nashua, NH). Three specimens were placed in a graphite crucible for each run. The binder burnout cycle for ZrB_2-based specimens was determined using thermogravimetric differential thermal analysis (SDT 2960 Simultaneous TG-DTA, TA Instruments, New Castle, DE) of PVP, which indicated significant weight loss beginning at 325 °C and ending at 480 °C in air. Removal of the binder from the formed samples occurred in an initial step at a heating rate of 4 °C/min to 600 °C with an isothermal hold of one hour in medium vacuum ($\sim 10^{-5}$ Torr) to obtain brown bodies. The sintering procedure, which was based off of previous sintering investigations [13], continued at a rate of 10 °C/min to 1650 °C for a 1-h hold at which point argon was flowed into the system. A final 10 °C/min ramp to 1850 °C for an isothermal hold of 1.5 h was performed in an inert argon environment to densify the ZrB_2 rings, followed by cooling to room temperature at 25 °C/min.

2.5. Characterization

A ZetaSizer Nano Z (Malvern Instruments, UK) was used to measure the electrokinetic potential (ζ in mV) of as-received ZrB_2, B_4C and WC powder particle surfaces in solutions of DI water with and without dispersant. As-received ZrB_2, B_4C and WC powders were combined to prepare a mixture with similar powder content as the attrition milled powders. Zeta potential curves at varying pH values of mixtures of as-received ZrB_2,

B_4C and WC powders and attrition milled powders in DI water with and without dispersant were also evaluated to determine the effect, if any, that attrition milling had on the zeta potential of the particle surfaces. 50-mL solutions were prepared by combining 0.05 wt% powders and DI water with or without 0.35 wt% dispersant and mixing the solutions using an ultrasonic probe (Branson Digital Sonifier, Model 250) for three minutes at 30% power output. The stock solutions were divided into two parts, and the pH was decreased using hydrochloric acid (HCl) or increased using sodium hydroxide (NaOH) to obtain zeta potential measurements at varying pH values. The pH of the solution was monitored using an Oakton PH5 meter (Vernon Hills, IL) calibrated with electrolytic buffer solutions at pHs of 4 and 10. Zeta potential measurements were taken at pH values ranging from ~2 to 13. Each zeta potential measurement of a set pH solution was an average of 50 total measurements.

An Anton Paar Modular Compact Rheometer (MCR) 302 (Ashland, VA) with a 25-mm profiled plate geometry and a gap of 1 mm was used to evaluate the rheological responses of the ZrB_2-based suspensions with varying powder and PVP contents at 25 °C. Because the viscosity of the suspensions was qualitatively paste-like, the profiled plate allowed for better contact between the suspension and the plate during testing. The shear rate applied to ZrB_2-based suspensions with PVP during room-temperature injection molding was estimated to be 3.15 s^{-1} by considering a sprue diameter of 3.175 mm and a compression rate of 75 mm/min applied by the MTS crosshead onto the suspension while forming. This approximate shear rate is much lower than that of conventional injection molding, which is typically on the order of 100–1000 s^{-1} [31]. As a result, the suspensions were ramped continuously to 100 s^{-1} and back to 0 s^{-1} to obtain preliminary flow curves. Flow startups in which a constant shear rate ranging from 0.01 s^{-1} to 100 s^{-1} was applied were performed to reveal the transient (i.e. time-dependent) response of the suspensions. Creep tests were ultimately utilized to evaluate the flow behavior in order to approximate the stress required to initiate flow of the suspensions. Creep tests involved applying a constant shear stress to a suspension and then measuring the shear rate response. Applied stress values ranged from 0.01 Pa up to 1100 Pa for 100 s to 300 s to determine the stress needed to cause a suspension to flow. The pH of suspensions was characterized using the previously mentioned Oakton PH5 meter.

After a ring-shaped ZrB_2 part was formed by room-temperature injection molding and dried, a polishing wheel with 320-, 400- and 600-grit silicon carbide grinding cloth (LECO 810-265/269-PRM) was used to machine the specimen in its green state to determine if PVP imparted sufficient strength to the parts prior to binder burnout. Binder burnout and pressureless sintering were then performed as described above in Section 2.4.

Brown (after binder burnout) and sintered densities of ZrB_2 rings were determined using the Archimedes technique [32]. The theoretical density of specimens containing ZrB_2, B_4C and WC was calculated using a rule-of-mixtures approach based on nominal batch formulations of attrition milled powders [13]. The calculated theoretical density was used as a comparison to determine how dense the ceramic specimens became after binder burnout and after pressureless sintering. Microstructural analysis was performed using an FEI Philips XL-40 scanning electron microscope (SEM) to examine sintered, polished and chemically etched (NaOH–water solution, 7 min) samples. Average grain size was calculated using the lineal intercept method [33] by evaluating five SEM micrographs for a particular sample composition and measuring the length of 50 arbitrary grains in each image using ImageJ image processing and analysis software. A total of 250 line segments representing 250 different grain lengths were averaged to obtain a mean grain size for each composition. Densities and grain sizes of samples prepared using suspensions of varying PVP content were compared using a two-tailed *t*-test to ascertain if respective data sets were statistically different [34]. The *p*-values calculated by the Student's *t*-test using the Excel function, *TTEST*, were deemed statistically different when $p < 0.05$. Energy dispersive spectroscopy (EDS) was utilized to qualitatively evaluate the elemental composition of sintered ZrB_2 cross-sections after polishing. As with the attrition milled powders, chemical analysis of sintered specimens was performed by NSL Analytical Services, Inc. (Cleveland, OH) to determine boron and tungsten contents using ICP-OES, carbon and oxygen contents by a Leco Furnace method and zirconium content by difference after the impurities scan. X-ray diffraction (XRD) using a Bruker D8 Focus X-Ray Diffractometer (Madison, WI) was also performed for phase analysis.

3. Results and discussion

3.1. Powder characteristics

3.1.1. Individual as-received powders

The plot comparing zeta potential versus pH for as-received ZrB_2, B_4C and WC powders is shown in Fig. 3. The isoelectric point (IEP) of ZrB_2 powder in water occurred at pH of 2.6, whereas the addition of the ammonium polyacrylate dispersant

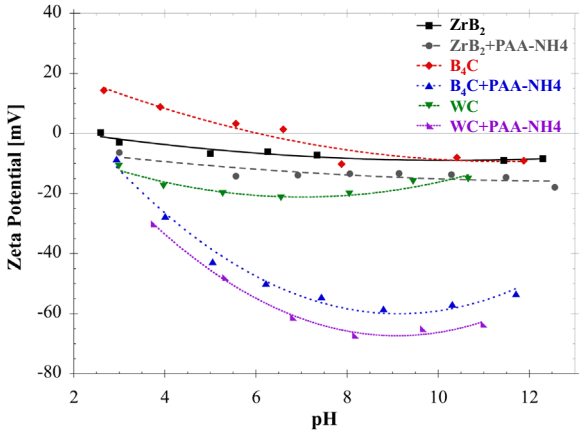

Fig. 3. Zeta potential curves of as-received ZrB_2, B_4C and WC powders in water with and without ammonium polyacrylate (PAA-NH4) dispersant.

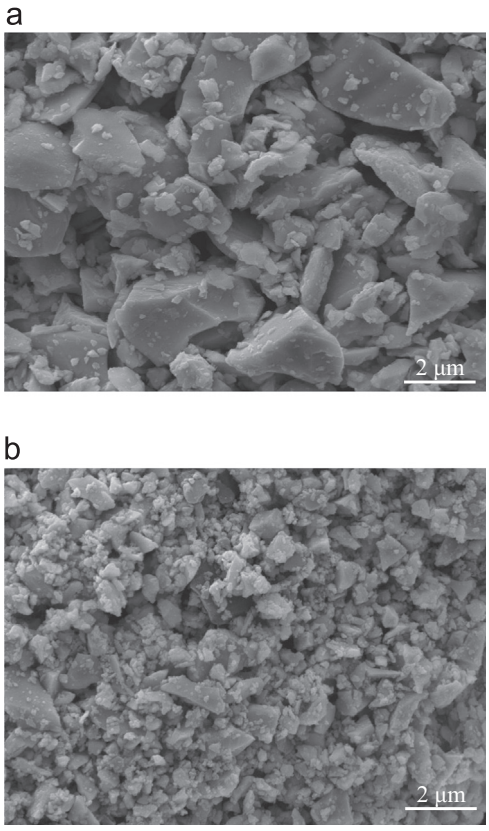

Fig. 4. SEM micrographs of (a) as-received ZrB_2 powders (H.C. Starck Grade B); (b) ZrB_2+B_4C powders after attrition milling with WC media resulting in $d_{50}\sim0.5$ μm.

decreased the pH at which the IEP occurred to pH∼1, which was also observed by a previous investigation [19] using a similar dispersant. As-received zirconium diboride powders in water exhibited a maximum negative zeta potential of −9.0 mV at pH of 11.4. The |ζ| of ZrB_2 over the pH range investigated increased slightly with the addition of dispersant such that a maximum negative zeta potential value of −18 mV was observed at pH∼12.6. This result suggested that while the dispersant enhanced the negative surface charge of the ZrB_2 particles, overall colloidal stability was still poor, as moderate colloidal stability is typically achieved at zeta potential values of at least |±30 mV| or higher [35]. Zeta potential measurements suggested that ZrB_2 powders were not readily dispersible in aqueous solutions even with addition of dispersant.

Curves of zeta potential versus pH for as-received B_4C powder displayed a notably different trend compared with those for ZrB_2 powder. The IEP of B_4C powder in water was observed at pH∼6, which matched a previous investigation [36], with a maximum |ζ| of −10 mV occurring at pH∼12. With the addition of dispersant, the estimated IEP shifted to pH∼2, and the magnitude of negative zeta potential increased significantly to −58 mV at pH∼8.8. This large increase in negative zeta potential magnitude indicated that the ammonium polyacrylate dispersant considerably enhanced the stability of B_4C powder in water.

WC powder exhibited the largest negative zeta potential compared to as-received ZrB_2 and B_4C powders in water without dispersant. A maximum negative zeta potential of −21 mV at pH∼6.6 was observed for the as-received WC powders in water. Negative zeta potential values of WC powders were greatly enhanced with the addition of dispersant. A maximum negative zeta potential of −67 mV, the highest magnitude of the three as-received powders, at pH∼8.1 was obtained, indicating that WC powders were the most stable in water with the addition of the dispersant out of the three powders investigated.

Table 2
Chemical analysis of attrition milled powders and sintered ZrB_2 specimens.

Wt%	Milled	Sintered specimen (46Z-2P)
O	2.1	0.003
C	1.5	0.3
W	7.2	9.5
Zr	69.7	68.7
B	17.4	19.1

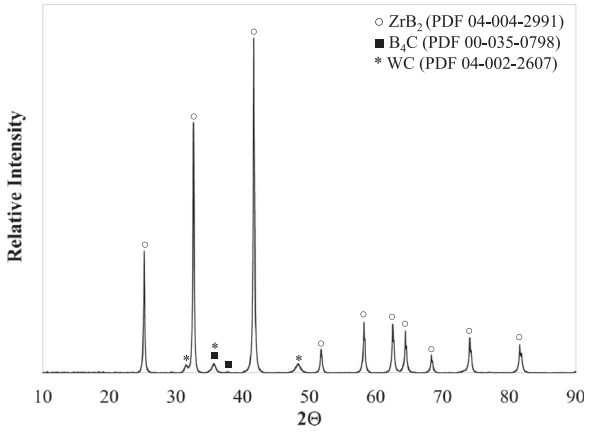

Fig. 5. XRD pattern of attrition milled powders.

3.1.2. Powder mixtures

Powder particles had an irregular shape before and after milling (refer to Fig. 4). SEM analysis confirmed that attrition milling effectively reduced the size of starting ZrB_2 and B_4C particles. The average particle size of attrition milled powders was determined to be ∼0.5 μm. Chemical analysis (presented in Table 2) indicated that there was 2.1 wt% oxygen content in the powders after attrition milling. Although oxygen content is undesirable in the powders, it was comparable to a study that attrition milled ZrB_2 and B_4C powders with WC milling media and achieved full density by pressureless sintering at 1850 °C [12]. The XRD pattern of attrition milled powders is shown in Fig. 5. The phases that were detected included ZrB_2, B_4C and WC. Oxygen-containing phases were not detected by XRD, which suggested that oxygen content was present in the form of a glass, likely ZrO_2 and/or B_2O_3 [12]. The composition of the attrition milled powder was estimated by measuring mass loss of attrition milling media to be 86 wt% ZrB_2, 3.5 wt% B_4C and 10.5 wt% WC, as approximately 22 g of WC was

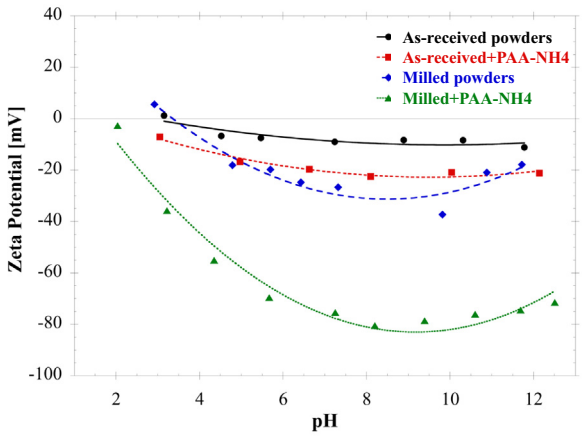

Fig. 6. Zeta potential curves of as-received and attrition milled ZrB_2, B_4C and WC powders in water with and without ammonium polyacrylate (PAA-NH4) dispersant.

introduced into a 200 g batch of ZrB_2–B_4C powders during attrition milling from the WC media. Although only ~8 wt% WC was initially desired to be incorporated into the powder mixture, WC content could be reduced to match previous studies [12,13] by further optimizing milling time and speed.

Zeta potential curves are shown in Fig. 6. The zeta potential curve for as-received powder mixtures of 86 wt% ZrB_2, 3.5 wt% B_4C and 10.5 wt% WC in aqueous solutions without and with ammonium polyacrylate dispersant indicated maximum $|\zeta|$ of −11.2 mV at pH of 11.8 and of −22.5 mV at pH of 8.1, respectively. The powder mixture that was attrition milled exhibited maximum negative zeta potentials of −37.3 mV at pH of 9.8 and −80.5 mV at pH ~ 8.2 in aqueous solutions without and with dispersant, respectively, which was comparable to a previous study [18]. Additionally, the isoelectric point (IEP) of the attrition milled powders shifted from pH ~ 3 to ~2 with the addition of ammonium polyacrylate.

Overall, magnitudes of maximum zeta potential were larger for attrition milled powders than for the as-received powder mixture or for any of the individual powders without dispersant, indicating that reducing particle size via attrition milling improved suspension stability of the particles in water, although not enough to promote effective stabilization. The zeta potential curve for the unmilled powder mixture matched closely that of as-received ZrB_2 powders in water, while the addition of dispersant resulted in slightly increased $|\zeta|$ values, which were still too low to achieve effective stabilization. With the ammonium polyacrylate addition, negative zeta potentials of attrition milled powders at varying pH values were significantly increased with a maximum $|\zeta|$ of −80.5 mV at pH of 8.2, indicating that the dispersant induced excellent stability in aqueous solutions. The general ζ trend of attrition milled powders matched that of the individual B_4C and WC powders more closely than that of ZrB_2 powders in water with dispersant. Consequently, B_4C and WC likely dominated the ζ behavior of the attrition milled powders in water with dispersant. This result implied that the sintering aids likely had a stabilizing effect on the attrition milled powder mixture with dispersant, yielding powders suitable for dispersion in water.

The high stability achieved with the attrition milled powders in water with ammonium polyacrylate dispersant facilitated powder loadings up to 49 vol% in aqueous suspensions. Because the concentrated suspensions contained three distinct powder phases with PVP in water dispersed with ammonium polyacrylate, the interparticle potential interactions could not be readily approximated as in a previous study of alumina-PVP suspensions [28], due to the complexity of the suspensions. Further analysis is needed to understand the character of the powders in aqueous solution with ammonium polyacrylate along with the added effect of PVP in these water-based, highly concentrated suspensions.

3.2. Characterization of aqueous ZrB_2-based suspensions

3.2.1. pH

The pH of suspensions loaded with 46 vol% of attrition milled 86 wt% ZrB_2, 3.5 wt% B_4C and 10.5 wt% WC powders (henceforth referred to as ZBW powders) with varying PVP content was 8.9 ± 0.3, while the pH of suspensions with 49 vol% ZBW powders with various PVP contents was 9.5 ± 0.2. The narrow range of pH values obtained for aqueous suspensions of attrition milled powders indicated that PVP did not greatly alter the pH. The pH of the ZrB_2-based suspensions used for forming was always higher than the IEP, suggesting that the powder particles had an overall negative surface charge. Furthermore, the pH of the suspensions was in the pH range where the magnitude of zeta potential of attrition milled powders in water with dispersant was maximized. Because the dispersant was comprised of ammonium polyacrylic acid, which was expected to fully dissociate at pHs > 8.5 [25], the dispersant was likely fully dissociated at the pH of the suspensions evaluated in this study. The dispersant appeared to effectively disperse the suspensions, so that no additional pH modification of suspensions was necessary to enhance dispersion for the purposes of this study.

3.2.2. Rheology

Start-up flow tests for suspensions of 46 vol% and 49 vol% ZBW powders with and without PVP were performed at constant shear rates of $0.01\ s^{-1}$ up to $100\ s^{-1}$. These tests revealed that all ZrB_2-based suspensions, regardless of PVP content, behaved in a time-dependent, viscoelastic manner, suggesting that the suspensions would not exhibit a steady-state yield stress. This transient, multifaceted flow behavior was likely the consequence of the complex particle interactions of three distinct powder phases, PVP and dispersant in the aqueous, highly concentrated suspensions. As a consequence, flow models, like Bingham or Herschel–Bulkley models, which were previously applied to PVP-alumina suspensions for room-temperature injection molding [27,28], could not be applied.

Creep tests were utilized to approximate the shear stresses required to initiate flow of ZrB_2-based suspensions. At low applied shear stresses, suspensions did not readily flow and

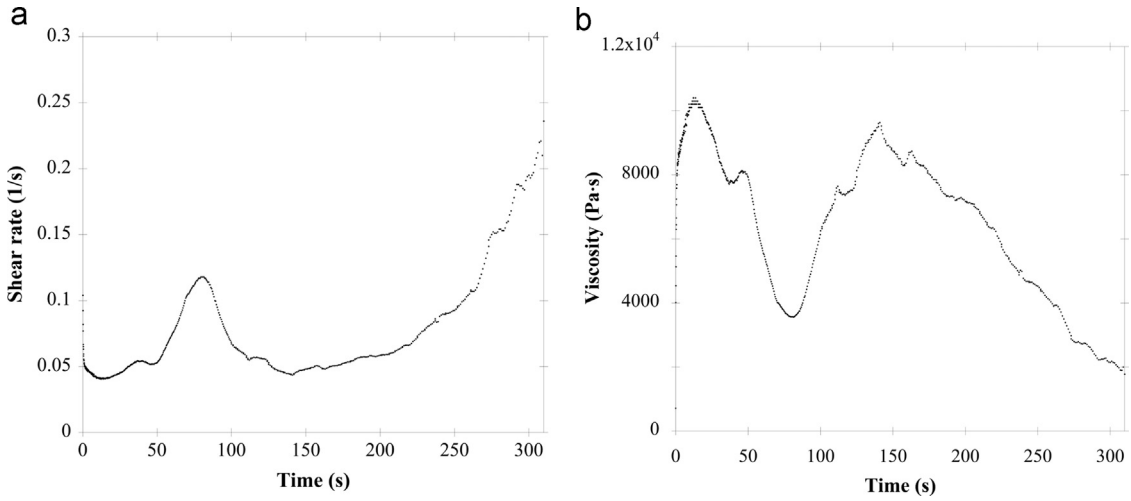

Fig. 7. Creep data at an applied stress of 420 Pa for a suspension containing 49 vol% ZBW and 2 vol% PVP plotted in terms of (a) shear rate vs. time and (b) viscosity vs. time.

exhibited a shear thickening response. However, the flow response transitioned to Newtonian-like flow and eventually to a shear-thinning response near a critical shear stress, above which suspensions exhibited a time-dependent, shear-thinning and thickening behavior depending on the time scale. Fig. 7 shows the typical behavior observed for a suspension during a creep test at an applied stress above its critical shear stress. Although a shear-thickening response is not desirable for most ceramic processing methods, it is believed that the time scale of room-temperature injection molding and the shear stress applied with aid from the pneumatic vibrator put ZrB_2-based suspensions into a flowable state allowing for adequate filling of the mold. The processability of the suspensions and resulting zirconium diboride specimens are discussed further in subsequent sections.

As shown in Table 1, suspensions containing 46 vol% ZBW powders required lower critical shear stresses to initiate flow in comparison with suspensions containing 49 vol% ZBW powders. The critical shear stress causing flow in the suspension of 46 vol% powders without polymer was 187 Pa, which then decreased to 52 Pa, the lowest flow stress value observed in the study, for suspensions containing 1 vol% PVP. At PVP contents at and above 2 vol%, the stress increased with PVP content. Suspensions of 49 vol% powders required overall higher stresses to initiate flow. Additionally, with increasing PVP content for suspensions containing 49 vol% powders, the stress required to cause flow increased from 389 Pa (no PVP) to approximately 567 Pa (1 vol% PVP) and then down to 235 Pa (3 vol% PVP). In suspensions containing 4 vol% PVP and above, the stress increased. The minimum critical shear stresses of 52 Pa and 235 Pa in suspensions of 46 vol% ZBW powder with 1 vol% PVP and 49 vol% ZBW powder with 3 vol% PVP, respectively, suggested that PVP may enhance dispersion in the suspensions at those concentrations. Furthermore, the dispersant was not likely present as a monolayer on the particle surfaces due to the high amount of dispersant present in the suspensions. The high dispersant content might have resulted in excess PAA-NH4 in the suspension and, thus, affected the flow properties of suspensions. Further analysis of suspensions containing higher concentrations of PVP and of varying molecular weight, as well as varying dispersant content, is needed to fully understand the complex flow behavior of aqueous ZrB_2-based suspensions evaluated in this study.

Although zeta potential measurements indicated maximum dispersion to occur at pH∼8.2 for solutions of attrition milled powders in water with dispersant, the magnitude of zeta potential of suspensions containing 46 vol% ZBW powder was likely nearly maximized at pH∼8.9. The pH∼9.5 of suspensions loaded with 49 vol% powder was slightly higher than the pH at which the maximum zeta potential magnitude occurred, suggesting that these suspensions might be less stable. The higher stresses needed to initiate flow in the suspensions observed in rheological characterization reflected this, as higher flow stresses are typically an indicator of colloidal instability [37]. However, the highly negative zeta potential at the pHs of ZBW-PVP suspensions indicated that suspensions were likely dispersed and stable for the purposes of this study.

3.3. Characterization of ZrB_2 specimens prepared by room-temperature injection molding

3.3.1. Processability and machinability prior to binder burnout and sintering

Ring-shaped specimens were successfully produced using ZrB_2-based suspensions of varying powder and PVP contents by the room-temperature injection molding process as previously adapted to an alumina system [27]. Suspensions containing 46 vol% ZBW powder and 1, 2, 3 and 4 vol% PVP, as well as suspensions of 49 vol% ZBW powder with 1, 2 and 3 vol% PVP, had suitable flow properties that yielded ZrB_2 rings without cracking during drying or removal from the mold. Suspensions of 46 vol% ZBW powder with 5 vol% PVP

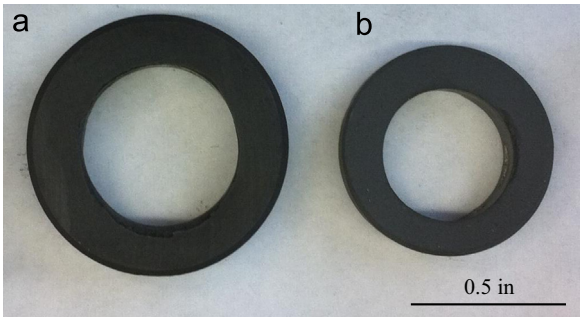

Fig. 8. ZrB_2 specimens produced by room-temperature injection molding (a) before and (b) after binder burnout and sintering.

and of 49 vol% ZBW powder with 4 or 5 vol% PVP did not have appropriate flow properties needed to effectively fill the ring-shaped mold. Specimens without significant defects, like pores or cracks, could not be prepared using these suspensions, which exhibited critical shear stresses >600 Pa needed to initiate flow (refer to Section 3.2.2).

Prior to binder burnout and sintering, specimen surfaces were ground using a polishing wheel by hand to even out planar surfaces of the rings. Specimens prepared from suspensions without PVP were too brittle after drying, and broke during mold removal or grinding, whereas all specimens prepared with suspensions containing PVP were effectively prepared without cracking or chipping during the grinding procedure. Thus, the minimal amount (≤ 5 vol%) of PVP used in suspensions imparted sufficient strength to specimens to allow for grinding prior to binder burnout and sintering.

3.3.2. Brown and sintered densities

The theoretical density (TD) of sintered specimens was calculated to be 6.17 g/cm^3 based on rule of mixtures. Brown (after binder removal) and sintered density values of the specimens prepared with suspensions of varying PVP and powder contents are presented in Table 1. After binder burnout, brown bodies formed with suspensions containing 46 vol% ZBW powders exhibited densities ~53%TD. Only the brown density of specimens prepared with suspensions containing 4 vol% PVP were statistically higher when compared with specimens of suspensions with 3 vol% PVP. The brown densities of specimens prepared with 49 vol% ZBW powders exhibited statistically higher brown densities of ~55%TD compared with the densities of specimens of suspensions with 46 vol% powder. This result suggested that the brown density of specimens increased with suspension powder loading, which implied better particle packing was attained, as would be expected with higher powder loadings in slurries [38]. Furthermore, PVP content did not appear to appreciably influence the brown density. Although brown densities of the rings were lower than those previously seen in alumina samples prepared by the same technique [27], the values were comparable to densities after binder removal obtained for ZrB_2 disks prepared by slip casting using aqueous suspensions with a citric-acid dispersant and additional pH modification [36].

Pressureless sintered specimens reached near full density regardless of initial PVP or powder content. Average densities for specimens prepared with suspensions containing 46 vol% ZBW powders were statistically similar at ~98%TD, whereas the average densities for specimens prepared with 49 vol% ZBW powder suspensions were statistically different. When comparing specimens prepared using suspensions of different powder loadings, sintered densities of specimens from suspension 49Z-3P were statistically the same at ~98%TD as all specimens of 46 vol% powder. Specimens produced using suspensions containing 1 vol% PVP, regardless of powder loading, were statistically similar at ~99%TD. Specimens formed using suspension 49Z-2P had the statistically highest average density of all specimens, suggesting that this suspension had optimal flow properties that possibly minimized pore formation, yielding specimens that could be fully densified after binder burnout and pressureless sintering.

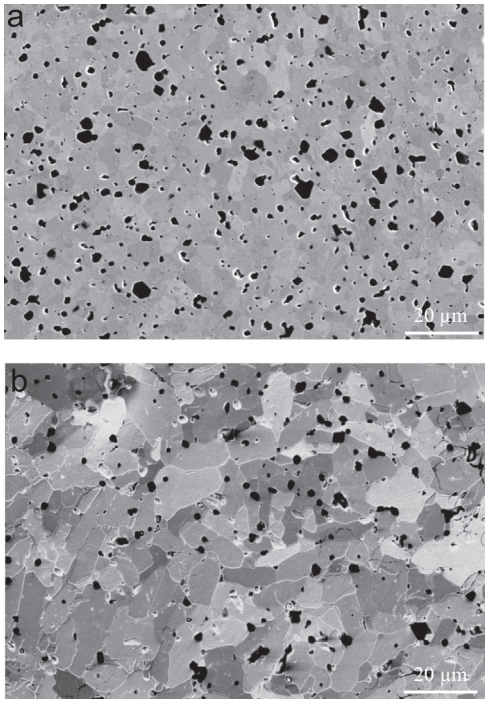

Fig. 9. SEM micrographs of representative cross-sections of sintered ZrB_2 specimens prepared by room-temperature injection molding (a) before and (b) after chemical etching. As shown in Fig. 10, the dark phases are likely boron carbide grains.

Specimens that underwent the heat treatment described in Section 2.4 to remove the binder and densify parts exhibited ~20% linear shrinkage regardless of initial PVP or powder content. Fig. 8 shows a typical ring before and after sintering. Because all specimens reached near full density, binder content and the higher-than-anticipated WC content did not appear to impede overall densification of ZrB_2 rings during pressureless sintering.

3.3.3. Microstructure and composition

SEM micrographs of polished and chemically etched cross-sections of sintered ZrB_2 rings indicated a dense microstructure with few pores between and within grains as shown in Fig. 9. Average grain sizes for specimens produced using varying PVP and powder loadings are shown in Table 1. All specimens had statistically similar grain sizes, except for specimens prepared with suspension 49Z-3P, which yielded

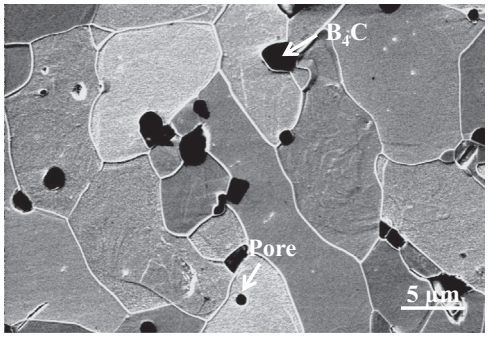

Fig. 10. Cross-section of specimen prepared using a suspension containing 1 vol% PVP with B_4C grain identified by EDS.

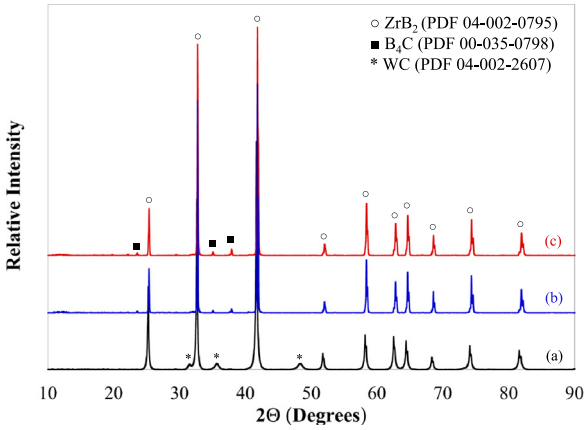

Fig. 11. XRD patterns of (a) attrition milled ZBW powders, sintered ZrB_2 specimens prepared with suspensions containing 3 vol% PVP and (b) 46 vol% ZBW powders and (c) 49 vol% ZBW powders.

specimens with statistically larger average grain sizes than those prepared by 46Z-2P and 46Z-4P. The cause of the difference in grain sizes for the specimens of 49Z-3P was unclear; however, because suspension 49Z-3P yielded specimens with larger grains, as well as lower sintered densities, compared to specimens of 49Z-2P, 49Z-3P appeared to impart inferior microstructural properties to specimens prepared with the suspension by room-temperature injection molding.

EDS revealed the presence of zirconium, boron and tungsten in sintered specimens as shown in Fig. 10. EDS point analysis suggested that the black grains were boron carbide, whereas the lighter gray grains were zirconium diboride with varying tungsten content, as highlighted in Fig. 10. Boron carbide grains appeared to be uniformly interspersed between ZrB_2 grains throughout specimen cross-sections. No pure tungsten or tungsten carbide phases were detected using EDS point analysis, likely because tungsten tends to dissolve into ZrB_2 at the elevated temperatures encountered during sintering, resulting in a solid solution of a tungsten-containing ZrB_2 phase [39].

XRD confirmed that the phases present in each specimen regardless of starting PVP content were ZrB_2 and B_4C after densification as shown in Fig. 11. Unlike with EDS, no signal from tungsten or tungsten carbide was detected by XRD in sintered specimens due to incorporation into the ZrB_2 lattice, in lines with previous studies [11,39,40]. Furthermore, no oxide phases, like zirconia, which would be expected if specimens were oxidized [40], were detected by XRD. Although if the oxide was present in its glassy state, it would not be detected using XRD. Consequently, chemical analysis detected 0.003 wt% oxygen (refer to Table 2). The negligible oxygen content further suggested that the binder burnout and pressureless sintering procedure, in combination with sintering aids, effectively eliminated oxygen from the starting powders and inhibited the formation of oxides in the final specimens.

4. Summary and conclusions

Room-temperature injection molding was effectively adapted to aqueous suspensions of attrition milled 86 wt% ZrB_2, 3.5 wt% B_4C and 10.5 wt% WC powders to produce dense, ring-shaped parts. Suspensions with 49 vol% ZBW powders with 1, 2 and 3 vol% PVP (MW = 10,000 g/mol) and suspensions of 46 vol% ZBW powders with 1, 2, 3 and 4 vol% PVP were flowable under the processing conditions. The pH value of ZBW suspensions with varying PVP content was ~8.9 for suspensions containing 46 vol% powder and ~9.5 for those containing 49 vol% solids, suggesting that powder content, not the amount of PVP, influenced the pH of suspensions. Zeta potential measurements of attrition milled powders suggested that the zeta potential magnitude was effectively maximized with ammonium polyacrylate dispersant in these pH ranges, requiring no additional pH modification of the suspensions.

ZrB_2 parts that resulted from room-temperature forming of ZrB_2-based suspensions containing PVP could be ground prior to binder removal and densification, suggesting that minimal PVP additions imparted sufficient green strength. Brown bodies with densities of ~56%TD were obtained for specimens prepared using suspensions of 49 vol% ZBW powder and 2 vol% PVP. After binder burnout and pressureless sintering, EDS, XRD and chemical analysis confirmed that no undesirable oxide phases developed within ZrB_2 parts, suggesting that processing of suspensions with PVP, dispersant and water did not alter the resulting composition of the ZrB_2 rings. Specimens reached near full density (>97%TD) regardless of powder or PVP content. Specimens prepared with suspensions containing 49 vol% ZBW powder and 2 vol% PVP had the highest relative densities (~100%TD). Additional analysis, including mechanical properties, is required to determine if the suspensions containing 49 vol% ZBW powder and 2 vol% PVP is an optimal composition for room-temperature injection molding of ZrB_2 specimens.

Room-temperature injection molding of aqueous ZrB_2-based suspensions has proven to be a feasible method to obtain dense ZrB_2 rings in an environmentally friendly way without the need for heating or complex chemical reactions. The ability to modify the flow properties using minimal PVP additions and ammonium polyacrylate dispersant will allow these versatile suspensions to be adapted to other novel, green processing methods for ultra-high temperature ceramics.

Acknowledgments

This work was funded by National Science Foundation Materials and Surface Engineering CMMI Grant 0726304, U. S. Department of Education GAANN Grant P200A10036 and Army Research Office Grant W911NF-13-1-0425. Additional support and access to resources at NASA Glenn Research Center were provided through the NASA Pathways Program. Thanks are due to Dr. Manuel Acosta for guidance and input throughout the investigation, Dr. Joe Grady for his support and valuable discussions, Prof. Kendra Erk and her research group for training and use of rheometric equipment, Dr. Bryan Harder and Dr. Richard Rogers for XRD assistance, Mr. Dereck Johnson for chemical analysis and Mr. Bob Angus and Mr. Gerald Hurd for sintering work.

References

[1] E. Wuchina, E.J. Opila, M. Opeka, W. Fahrenholtz, I. Talmy, UHTCs: Ultra-High Temperature Ceramic materials for extreme environment applications, Electrochem. Soc. Interface 16 (2007) 30–36.
[2] D.M. Van Wie, D.G. Drewry Jr., D.E. King, C.M. Hudson, The hypersonic environment: required operating conditions and design challenges, J. Mater. Sci. 39 (2004) 5915–5924.
[3] E.L. Corral, R.E. Loehman, Ultra-high-temperature ceramic coatings for oxidation protection of carbon–carbon composites, J. Am. Ceram. Soc. 91 (2008) 1495–1502.
[4] S.R. Levine, E.J. Opila, M.C. Halbig, J.D. Kiser, M. Singh, J.A. Salem, Evaluation of ultra-high temperature ceramics for aeropropulsion use, J. Eur. Ceram. Soc. 22 (2002) 2757–2767.
[5] L. Scatteia, F. Monteverde, D. Alfano, G. Marino, S. Cantoni, Advances in ultra high temperature ceramics for hot structures, Trans. Space Technol. Jpn. 7 (2009) 73–78.
[6] H. Pastor, Metallic Borides: Preparation of Solid Bodies—Sintering Methods and Properties of Solid Bodies, Boron and Refractory Borides, Springer, Berlin, Heidelberg, 1977, p. 457–493.
[7] S.-Q. Guo, Densification of ZrB_2-based composites and their mechanical and physical properties: a review, J. Eur. Ceram. Soc. 29 (2009) 995–1011.
[8] Y.-M. Chiang, W.D. Kingery, D.P. Birnie, Physical Ceramics: Principles for Ceramic Science and Engineering, J. Wiley, 1997.
[9] F. Monteverde, A. Bellosi, L. Scatteia, Processing and properties of ultra-high temperature ceramics for space applications, Mater. Sci. Eng. A 485 (2008) 415–421.
[10] R. Licheri, R. Orrù, C. Musa, G. Cao, Combination of SHS and SPS techniques for fabrication of fully dense ZrB_2–ZrC–SiC composites, Mater. Lett. 62 (2008) 432–435.
[11] A.L. Chamberlain, W.G. Fahrenholtz, G.E. Hilmas, Pressureless sintering of zirconium diboride, J. Am. Ceram. Soc. 89 (2006) 450–456.
[12] S.C. Zhang, G.E. Hilmas, W.G. Fahrenholtz, Pressureless densification of zirconium diboride with boron carbide additions, J. Am. Ceram. Soc. 89 (2006) 1544–1550.
[13] W.G. Fahrenholtz, G.E. Hilmas, S.C. Zhang, S. Zhu, Pressureless sintering of zirconium diboride: particle size and additive effects, J. Am. Ceram. Soc. 91 (2008) 1398–1404.
[14] Z. Lü, D. Jiang, J. Zhang, Q. Lin, Microstructure and mechanical properties of zirconium diboride obtained by aqueous tape casting process and hot pressing, J. Am. Ceram. Soc. 93 (2010) 4153–4157.
[15] C. Tallon, D. Chavara, A. Gillen, D. Riley, L. Edwards, S. Moricca, G.V. Franks, Colloidal processing of zirconium diboride ultra-high temperature ceramics, J. Am. Ceram. Soc. 96 (2013) 2374–2381.
[16] V. Medri, P. Pinasco, A. Sanson, E. Roncari, S. Guicciardi, A. Bellosi, ZrB_2-based laminates produced by tape casting, Int. J. Appl. Ceram. Technol. 9 (2012) 349–357.
[17] S.L. Natividad, V.R. Marotto, L.S. Walker, D. Pham, W. Pinc, E.L. Corral, Tape casting thin, continuous, homogenous, and flexible tapes of ZrB_2, J. Am. Ceram. Soc. 94 (2011) 2749–2753.
[18] T. Huang, G.E. Hilmas, W.G. Fahrenholtz, M.C. Leu, Dispersion of zirconium diboride in an aqueous, high-solids paste, Int. J. Appl. Ceram. Technol. 4 (2007) 470–479.
[19] Z. Lü, D. Jiang, J. Zhang, Q. Lin, Aqueous tape casting of zirconium diboride, J. Am. Ceram. Soc. 92 (2009) 2212–2217.
[20] Z. Lü, D. Jiang, J. Zhang, Q. Lin, Processing and properties of ZrB_2–SiC composites obtained by aqueous tape casting and hot pressing, Ceram. Int. 37 (2011) 293–301.
[21] V. Medri, C. Capiani, A. Bellosi, Properties of slip-cast and pressureless-sintered ZrB_2–SiC composites, Int. J. Appl. Ceram. Technol. 8 (2011) 351–359.
[22] R. He, X. Zhang, P. Hu, C. Liu, W. Han, Aqueous gelcasting of ZrB_2–SiC ultra high temperature ceramics, Ceram. Int. 38 (2012) 5411–5418.
[23] M.A. Janney, O.O. Omatete, C.A. Walls, S.D. Nunn, R.J. Ogle, G. Westmoreland, Development of low-toxicity gelcasting systems, J. Am. Ceram. Soc. 81 (1998) 581–597.
[24] M. Acosta, A.N.D. DESIGN, Manufacture of Ultra-High Temperature Ceramics with Oriented Strengthening and Toughening Phases, School of Materials Engineering, Purdue University, West Lafayette, IN, 2012.
[25] J. Cesarano III, I.A. Aksay, Processing of highly concentrated aqueous alpha-alumina suspensions stabilized with polyelectrolytes, J. Am. Ceram. Soc. 71 (1988) 1062–1067.
[26] R.T. Vanderbilt Company, Darvan 821A Technical Data Sheet, 2009.
[27] V.L. Wiesner, J.P. Youngblood, R.W. Trice, Room-temperature injection molding of aqueous alumina-polyvinylpyrrolidone suspensions, J. Eur. Ceram. Soc. 34 (2014) 453–463.
[28] M. Acosta, V.L. Wiesner, C.J. Martinez, R.W. Trice, J.P. Youngblood, Effect of polyvinylpyrrolidone additions on the rheology of aqueous, highly loaded alumina suspensions, J. Am. Ceram. Soc. 96 (2013) 1372–1382.
[29] L.M. Rueschhoff, M.J. Michie, W.J. Costakis, A.I. Diaz-Cano, J.P. Youngblood, R.W. Trice, Additive manufacturing of complex-shaped ceramic parts via room-temperature robocasting of alumina ceramic suspension gels (CeraSGels), (2015) in preparation.
[30] J.P. Beaumont, R. Nagel, R. Sherman, Successful Injection Molding, Hanser Gardner Publications, Inc., Cincinnati, 2002.
[31] B.C. Mutsuddy, R.G. Ford, Ceramic Injection Molding, 1st ed., Chapman & Hall, London, 1995.
[32] ASTM C 373-88, Standard Test Method for Water Absorption, Bulk Density, Apparent Porosity, and Apparent Specific Gravity of Fired Whiteware Products, ASTM International, West Conshohocken, PA, 2006.
[33] W.D. Kingery, H.K. Bowen, D.R. Uhlmann, Introduction to Ceramics, Wiley, New York, 1976.
[34] D.C. Montgomery, G.C. Runger, N.F. Hubele, Engineering Statistics, Wiley, 2007.
[35] R.J. Hunter, R.H. Ottewill, R.L. Rowell, Zeta Potential in Colloid Science: Principles and Applications, Academic Press, 2013.
[36] S. Leo, C. Tallon, G.V. Franks, Aqueous and nonaqueous colloidal processing of difficult-to-densify ceramics: suspension rheology and particle packing, J. Am. Ceram. Soc. 97 (2014) 3807–3817.
[37] R.G. Larson, The Structure and Rheology of Complex Fluids, Oxford University Press, New York, 1999.
[38] B.V. Velamakanni, F.F. Lange, Effect of interparticle potentials and sedimentation on particle packing density of bimodal particle distributions during pressure filtration, J. Am. Ceram. Soc. 74 (1991) 166–172.
[39] P.S. Kisliy, M.A. Kuzenkova, O.V. Zaveruha, On the sintering process of zirconium diboride with tungsten, Phys. Sint. 3 (1971) 29–44.
[40] S.C. Zhang, G.E. Hilmas, W.G. Fahrenholtz, Improved oxidation resistance of zirconium diboride by tungsten carbide additions, J. Am. Ceram. Soc. 91 (2008) 3530–3535.